

# Corneal Cross-Linking with Riboflavin and UV-A in the Mouse Cornea in Vivo: Morphological, Biochemical, and Physiological Analysis

Sabine Kling<sup>1,2\*</sup>, Arthur Hammer<sup>1\*</sup>, Alain Conti<sup>1</sup>, and Farhad Hafezi<sup>1,2,3,4</sup>

<sup>1</sup> Laboratory of Ocular Cell Biology, University of Geneva, Geneva, Switzerland

<sup>2</sup> Center for Applied Biotechnology and Molecular Medicine (CABMM), University of Zurich, Zurich, Switzerland

<sup>3</sup> Department of Ophthalmology, University of Southern California, Los Angeles, CA, USA

<sup>4</sup> ELZA Institute, Dietikon/Zurich, Switzerland

**Correspondence:** Sabine Kling, CABMM, University of Zurich, Winterthurerstrasse 190, 8057 Zurich, Switzerland. e-mail: kling.sabine@gmail.com

**Received:** 22 July 2016

**Accepted:** 11 December 2016

**Published:** 30 January 2017

**Keywords:** corneal cross-linking; UV irradiation; efficacy; mouse model

**Citation:** Kling S, Hammer A, Conti A, Hafezi F. Corneal cross-linking with riboflavin and UV-A in the mouse cornea in vivo: morphological, biochemical, and physiological analysis. *Trans Vis Sci Tech.* 2017; 6(1):7, doi:10.1167/tvst.6.1.7

**Purpose:** To morphologically, biochemically, and physiologically characterize corneal cross-linking with riboflavin and UV-A light (CXL) in a newly established in vivo murine model.

**Methods:** C57BL/6 wild-type mice ( $N = 67$ ) were treated with various CXL protocols, with modification of the following parameters: total energy (fluence) used, duration of UV-A irradiation, continuous versus pulsed irradiation, and CXL under hypoxic conditions (contact lens). Corneas were evaluated biomicroscopically, histologically, and using optical coherence tomography. Conformational collagen changes were evaluated via changes in the speed of enzymatic digestion.

**Results:** A fluence of 5.4 J/cm<sup>2</sup> induced scar formation, while fluences of < 0.18 J/cm<sup>2</sup> induced neovascularization. Fluences between 1.62 and 2.7 J/cm<sup>2</sup> reduced epithelial thickness, but maintained a transparent cornea after 1 month. Pulsed UV irradiation inhibited neovascularization, but favored scar formation. Changes in the speed of enzymatic digestion suggest that CXL in mice, when compared to humans, requires less UV-A energy than the difference in corneal thickness between the species would suggest.

**Conclusions:** We demonstrated the in vivo response of very strong and very weak CXL and identified the best suited range of UV fluence in murine corneas. The presented murine CXL model may be helpful in future research addressing cellular and molecular pathways associated to CXL treatment.

**Translational Relevance:** Adverse tissue reactions following CXL treatment were observed, if the administered UV energy was out of the treatment window—raising concern about novel CXL treatment protocols that have not been previously validated in an experimental setting.

## Introduction

Corneal cross-linking (CXL) has become a powerful technique for the prevention of keratoconus progression in adults, children, and adolescents.<sup>1–4</sup> Its ability to increase the corneal stiffness is also of interest in treating<sup>5</sup> or regularizing<sup>6</sup> corneal ectasia after refractive surgery.<sup>5–7</sup>

The standard CXL treatment has been modified over the last few years, moving towards shorter treatment times, reduced patient discomfort, faster recovery periods, and an applicability to a wider

range of patients. Modified treatment protocols include accelerated CXL,<sup>8</sup> iontophoresis CXL,<sup>9</sup> trans-epithelial CXL,<sup>10</sup> hypoosmolar CXL,<sup>11</sup> pulsed CXL,<sup>12</sup> and contact lens-assisted CXL.<sup>13</sup> However, many of these approaches did not work as postulated,<sup>14–17</sup> mainly because the working principle behind CXL is largely unknown. A better understanding of CXL on the molecular level is required in order to optimize the treatment parameters.

While it is important to measure the ex vivo macroscopic stiffening effect with different CXL protocols, either by enzymatic digestion<sup>18</sup> or stress-strain biomechanical characterization,<sup>19–22</sup> in vivo

measurements are even more desired. A difficulty, however, is that mechanical parameters can only be estimated vaguely in vivo,<sup>23,24</sup> which is why long-term studies of corneal stiffness-evolution after CXL treatment have not been performed in a clinical setting yet.

Clinical studies show that CXL prevents keratoconus progression for more than 10 years.<sup>25</sup> This long-term increase in corneal stiffness, but also long-term geometrical corneal remodelling after CXL, potentially suggests that gene expression is likely to be affected, which is further supported by the fact that CXL is able to stop keratoconus—a disease with known alterations in protein production. Nevertheless, as CXL also decreases the speed of enzymatic digestion,<sup>18</sup> it is yet too early to rule out that the long-term stabilizing effect does not only result from decreased collagen degradation.

CXL has an immediate stiffening effect on the corneal tissue<sup>20,22</sup> and may potentially activate mechanotransductive processes. Mechanotransduction describes the mechanism of converting mechanical forces into biochemical signals (e.g., by unraveling proteins and exposing molecular recognition sites).<sup>26,27</sup> Resulting functional changes include cellular processes, such as migration, proliferation, and differentiation, but also protein production.<sup>27</sup> Mechanical forces between cells and the extracellular matrix (ECM) resulting from a change in the stress distribution may therefore induce important regulatory mechanisms, which in turn remodel the ECM and reorganize the tissue.<sup>28</sup>

In a recent study, we characterized the biomechanical changes induced by CXL in the murine cornea<sup>29</sup>; in the current study, we will analyze the morphological and physiological response of the murine corneal tissue following different CXL protocols. Characterizing the newly established mouse model for CXL will be a first step towards better understanding the molecular pathways involved in CXL in a healthy organism.

## Methods

### CXL Parameters

In order to transfer the CXL protocol from human to mouse, different assumptions were tested to determine the appropriate riboflavin concentration and UV energy. In all adapted CXL protocols, the treatment parameters were designed so that the

endothelial UV absorption was equal or less than in the human cornea under standard Dresden CXL.

We used the Lambert-Beer law to estimate the treatment parameters. The following reasoning was behind the different conditions: (1) If a certain amount of UV energy is required to induce cross-links in the corneal tissue, then in order to absorb the same energy dose along the mouse and human cornea, a higher riboflavin concentration is needed in the former. (2) In contrast, if a certain density of absorbed UV energy is required to induce the cross-links, then a higher riboflavin concentration and a lower UV energy dose is needed in the mouse cornea.

In another condition, we applied empirical estimations to determine the treatment parameters: (3) If the formation of cross-links in the human cornea is limited by oxygen diffusion, then both, riboflavin concentration and UV energy can be reduced in comparison to conditions (1) and (2), as the oxygen diffusion in the (thinner) mouse cornea is higher.

Additionally, in order to study the oxygen dependency in more detail, we included the following conditions: (4) different irradiation durations at constant fluence, (5) pulsed UV-light to increase oxygen availability, and (6) reduction of available oxygen in the stroma via placement of a contact lens.

### Same Absolute UV Absorption (i.e. Same Fluence)

As a mouse cornea is approximately 20% the thickness of a human cornea (114  $\mu\text{m}$ <sup>30</sup> versus 578  $\mu\text{m}$ <sup>31</sup>), the standard Dresden cross-linking protocol was adapted to obtain a similar absorption profile along the mouse cornea and the same threshold of 0.18 mW/cm<sup>2</sup> at the endothelium. The Lambert-Beer law describes the light absorption along the cornea:

$$\frac{I_{\text{endo}}}{I_0} = 10^{-\varepsilon_M \cdot C_M \cdot th} \quad (1)$$

where  $I_{\text{endo}}$  is the intensity at the endothelium,  $I_0$  is the intensity of the light source,  $\varepsilon_M = 10,066 \text{ L}/(\text{mol} \cdot \text{cm})$  is the molar extinction coefficient of riboflavin,  $C_M = 2.65 \text{ mmol/L}$ ,  $7.17 \text{ mmol/L}$ , and  $13.3 \text{ mmol/L}$  ( $\triangleq 0.1\%$ ,  $0.27\%$ ,  $0.5\%$  riboflavin) is the molar concentration of the riboflavin solution, and  $th$  is the mean corneal thickness. As the absorption coefficient of the unsaturated corneal stroma is about 10 times smaller than the absorption coefficient of riboflavin, the stromal UV absorption has not been considered in this approach. In order to get the same absolute absorption along the murine as the human

cornea,  $C_M$  of the murine riboflavin solution needs to be increased (given that  $\varepsilon$  does not change) by factor

$$\frac{th_{human}}{th_{mouse}} \approx 5 \quad (2)$$

where  $th_{mouse}$  is the stromal thickness of the murine cornea and  $th_{human}$  the minimally required<sup>32</sup> stromal thickness for CXL treatment. The parameters resulting from this approach were: 0.5% riboflavin solution and normal fluence (referred to humans) of 5.4 J/cm<sup>2</sup>, such as irradiation with 3 mW/cm<sup>2</sup> for 30 minutes. A total of 38 murine corneas were treated with 5.4 J/cm<sup>2</sup> and analyzed at 24 hours, 72 hours, and 1 month with different techniques (see Table 1).

### Same Relative UV Absorption (i.e., Same Fluence per Thickness)

To achieve a similar energy density absorbed by the cornea, the ratio of absorbed UV energy and corneal thickness must be constant. We derived the following two equations from the Lambert-Beer law to adjust the treatment parameters: The desired net UV energy absorbed by the cornea at a certain irradiance depends on the maximal allowed UV-threshold at the endothelium and can be calculated with equation 3. The required riboflavin concentration in the stroma to allow for this UV absorption can be calculated with equation 4.

$$E_{mouse} = E_{endo} + (E_0 - E_{endo}) \cdot \frac{th_{mouse}}{th_{human}} \quad (3)$$

$$C_{mouse} = \frac{\log_{10} \frac{E_{endo}}{E_{mouse}}}{-\varepsilon_M \cdot th_{mouse}} \quad (4)$$

where  $E_{mouse}$  is the net UV energy absorbed by the cornea,  $E_0$  is the nominal energy provided by the UV lamp,  $E_{endo}$  is the UV energy absorbed by the endothelium, and  $th_{mouse}$  and  $th_{human}$  are the mean corneal thicknesses in mice and humans, respectively. The resulting parameters from this approach were: 0.27% riboflavin solution and a fluence of 1.53 J/cm<sup>2</sup>, such as 9 mW/cm<sup>2</sup> for 2:50 minutes. A total of 11 murine corneas were treated with 1.53 J/cm<sup>2</sup> and analyzed at 24 hours and 1 month (Table 1).

### Minimal UV Irradiance to Induce Cross-Links

In order to determine the minimal irradiance needed to induce cross-links in the murine cornea, we tested the following empirical conditions:

0.1% riboflavin: 3 minutes at 3 mW/cm<sup>2</sup>, 1 minute at 3 mW/cm<sup>2</sup>, 30 seconds at 3 mW/cm<sup>2</sup>, 5 minutes at 500  $\mu$ W/cm<sup>2</sup>, and 6 minutes at 250  $\mu$ W/cm<sup>2</sup>; 0.27%

riboflavin: 3 minutes at 3 mW/cm<sup>2</sup>; 0.5% riboflavin: 2:30 minutes at 18 mW/cm<sup>2</sup> and 9 minutes at 3 mW/cm<sup>2</sup>.

A total of 48 murine corneas were treated with decreasing irradiances and analyzed at 24 hours, 72 hours, 7 days, and 1 month with different techniques (see Table 1).

### Effect of Irradiation Time

To study the effect of irradiation time, we included different conditions with the same fluence, but with different irradiances: 5.4 J/cm<sup>2</sup> at 3 mW/cm<sup>2</sup> ( $n = 15$ ), 9 mW/cm<sup>2</sup> ( $n = 12$ ), and 18 mW/cm<sup>2</sup> ( $n = 12$ ); 0.09 J/cm<sup>2</sup> at 250  $\mu$ W/cm<sup>2</sup> ( $n = 8$ ) and 3 mW/cm<sup>2</sup> ( $n = 10$ ).

### Pulsed Cross-Linking (pCXL)

Pulsed UV-light was applied in order to avoid hypoxia during UV irradiation. It is important to provide UV flashes that are distinctly shorter than the pauses of the interval.<sup>33</sup> We developed a protocol for the mouse cornea, where 100 ms UV-flashes with an irradiance of 100 mW/cm<sup>2</sup> were applied at a frequency of 1 Hz for 8:30 minutes, corresponding to a fluence of 0.54 J/cm<sup>2</sup>. Riboflavin was used at 0.27%. Three murine corneas were used to ascertain pulsed CXL.

### Contact Lens Assisted Cross-Linking (caCXL)

caCXL has the opposite effect of pCXL (i.e., it reduces the amount of available oxygen within the corneal tissue and hence leads to a lower amount of inducible free radicals). For caCXL, a contact lens (−0.5 D, SoftLens daily disposable, without UV filter, Bausch & Lomb, Inc., Rochester, NY) was reduced in size (3 mm diameter) and placed on top of the cornea during UV irradiation. In order to improve adhesion, a drop of riboflavin solution was used to humidify the cornea before applying contact lens. A 0.54-J/cm<sup>2</sup> fluence protocol was used, with 0.27% riboflavin, 3 mW/cm<sup>2</sup> irradiance, and 3-minute irradiation time. Six murine corneas were used to study contact lens assisted CXL.

### Control Conditions

Two control conditions were studied. “Virgin” corneas were left untreated. “Riboflavin” corneas were de-epithelialized, and riboflavin solution was instilled for 20 minutes. A total of 27 murine corneas were used for control conditions and analyzed at 24 hours, 72 hours, 7 days, and 1 month with different techniques (see Table 1). UV-only controls have not been included in this study due to ethical reasons.

**Table 1.** Summary of Treatment Conditions and Numbers of Eyes Analyzed with Different Measurement Techniques

| CXL Treatment/<br>Condition  | Riboflavin<br>(%) | Fluence<br>(J/cm <sup>2</sup> ) | Time of<br>Analysis | Total<br>Number of<br>Eyes | Total<br>Number of<br>Eyes/Condition | Slit Lamp<br>Inspection | OCT | Histology | Enzymatic<br>Digestion | Observation at 1 mo  |
|--|-------------------|---------------------------------|---------------------|----------------------------|--------------------------------------|-------------------------|-----|-----------|------------------------|--|
|  |                   |                                 |                     |                            |                                      |                         |     |           |                        |  |
| <b>Same absolute UV absorption (i.e., same fluence) as in the human cornea</b> |                   |                                 |                     |                            |                                      |                         |     |           |                        |  |
| 3 mW 30 min  | 0.5               | 5.4                             | 24 h                | 6                          | 15                                   | ✓                       | ✓   | ✓         | —                      | White, central scar, full biomechanical stiffening <sup>36</sup>                         |
| 9 mW 10 min  | 0.5               | 5.4                             | 24 h                | 3                          | 12                                   | —                       | —   | —         | ✓                      | White, central scar, full biomechanical stiffening <sup>36</sup>                         |
|  |                   |                                 | 1 mo                | 6                          |                                      | ✓                       | —   |           |                        |  |
|  |                   |                                 | 24 h                | 6                          |                                      | ✓                       | —   |           |                        |  |
| 18 mW 5 min  | 0.5               | 5.4                             | 24 h                | 6                          | 12                                   | ✓                       | ✓   | ✓         | —                      | White, central scar, full biomechanical stiffening <sup>36</sup>                         |
|  |                   |                                 | 1 mo                | 6                          |                                      | ✓                       | ✓   | —         |                        |  |
| <b>Same relative UV absorption (i.e., same fluence per thickness)</b>          |                   |                                 |                     |                            |                                      |                         |     |           |                        |  |
| 9 mW 2:50 min  | 0.27              | 1.53                            | 24 h                | 2                          | 11                                   | —                       | —   | ✓         | —                      | White, central scar, full biomechanical stiffening <sup>36</sup>                         |
|  |                   |                                 | 1 mo                | 9                          |                                      | ✓                       | —   | —         |                        |  |
| <b>Determining the minimal UV irradiance to induce cross-links</b>             |                   |                                 |                     |                            |                                      |                         |     |           |                        |  |
| 18 mW 2:30 min   | 0.5               | 2.7                             | 1 mo                | 4                          | 4                                    | —                       | —   | ✓         | —                      | Reduced epithelial thickness   |
| 3 mW 9 min   | 0.1               | 1.62                            | 1 mo                | 4                          | 4                                    | —                       | —   | ✓         | —                      | Reduced epithelial thickness, full biomechanical stiffening <sup>36</sup>                |
| 3 mW 3 min   | 0.27              | 0.54                            | 72 h                | 3                          | 5                                    | —                       | —   | —         | ✓                      | Epithelial abnormalities, full biomechanical stiffening <sup>36</sup>                    |
|  |                   |                                 | 7 d                 | 2                          |                                      | —                       | ✓   | —         |                        |  |
| 3 mW 1 min   | 0.1               | 0.18                            | 24 h                | 2                          | 9                                    | —                       | —   | ✓         | —                      | Immunologic reaction, neovascularization, reduced biomechanical stiffening <sup>36</sup> |
|  |                   |                                 | 72 h                | 3                          |                                      | —                       | —   | ✓         | —                      |  |
|  |                   |                                 | 1 mo                | 4                          |                                      | ✓                       | ✓   | —         |                        |  |
| 3 mW 30 s  | 0.1               | 0.09                            | 24 h                | 4                          | 10                                   | ✓                       | —   | ✓         | —                      | Immunologic reaction, neovascularization, reduced biomechanical stiffening               |

Table 1. Continued.

| CXL Treatment/<br>Condition       | Riboflavin<br>(%) | Fluence<br>(J/cm <sup>2</sup> ) | Time of<br>Analysis | Total<br>Number<br>of Eyes | Total<br>Number of<br>Eyes/Condition | Slit Lamp<br>Inspection | OCT | Histology | Enzymatic<br>Digestion | Observation at 1 mo  |
|-----------------------------------|-------------------|---------------------------------|---------------------|----------------------------|--------------------------------------|-------------------------|-----|-----------|------------------------|--|
| 72 h                              | 3                 | —                               | —                   | —                          | ✓                                    |                         |     |           |                        |  |
| 1 mo                              | 3                 | ✓                               | —                   | ✓                          | —                                    |                         |     |           |                        |  |
| 500 μW 5 min                      | 0.1               | 0.15                            | 24 h                | 4                          | 8                                    | ✓                       | —   | ✓         | —                      | Immunologic reaction,<br>neovascularization,<br>reduced<br>biomechanical<br>stiffening |
|                                   |                   |                                 | 1 mo                | 4                          |                                      | ✓                       | ✓   | ✓         | —                      |  |
| 250 μW 6 min                      | 0.1               | 0.09                            | 24 h                | 4                          | 8                                    | ✓                       | —   | ✓         | —                      | Immunologic reaction,<br>neovascularization,<br>reduced<br>biomechanical<br>stiffening |
|                                   |                   |                                 | 1 mo                | 4                          |                                      | ✓                       | —   | ✓         | —                      |  |
| <b>CXL with oxygen modulation</b> |                   |                                 |                     |                            |                                      |                         |     |           |                        |  |
| caCXL                             | 0.27              | 0.54                            | 1 mo                | 3                          | 6                                    | ✓                       | —   | ✓         | —                      | Immunologic reaction,<br>neovascularization,<br>reduced<br>biomechanical<br>stiffening |
|                                   |                   |                                 | 72 h                | 3                          |                                      | —                       | —   | —         | ✓                      |  |
| pCXL                              | 0.27              | 0.54                            | 1 mo                | 3                          | 3                                    | ✓                       | —   | ✓         | —                      | White, central scar  |
| <b>Control conditions</b>         |                   |                                 |                     |                            |                                      |                         |     |           |                        |  |
| ribo                              | 0.5               | —                               | 24 h                | 5                          | 16                                   | ✓                       | ✓   | ✓         | —                      | No adverse effects   |
|                                   | 0.27              | —                               | 72 h                | 3                          |                                      | —                       | —   | —         | ✓                      |  |
|                                   | 0.27              | —                               | 7 d                 | 2                          |                                      | —                       | —   | ✓         | —                      |  |
|                                   | 0.5               | —                               | 1 mo                | 6                          |                                      | ✓                       | ✓   | ✓         | —                      |  |
| virgin                            | —                 | —                               | —                   | 9                          | 11                                   | ✓                       | ✓   | ✓         | ✓                      | —  |
| virgin de-<br>epithelialized      | —                 | —                               | 7 d                 | 2                          |                                      | —                       | —   | —         | —                      | —  |

Full biomechanical stiffening refers to the maximally observed corneal strengthening; reduced biomechanical stiffening refers to a significantly lower than maximal corneal stiffening, but still significantly higher than control corneas.<sup>36</sup>

## Treatment Protocol

Sixty-seven adult male C57BL/6 wild-type mice were obtained from Charles River Laboratories (Research Models and Services, Bois des Oncins, France) and divided into the treatment conditions depicted in Table 1. The experiments were approved by the local ethical committee (Commission Cantonale pour les Expériences sur les Animaux [CCEA], Geneva, Switzerland and the Office Fédéral de la Sécurité Alimentaire et des Affaires Vétérinaires, Switzerland) and adhered to the ARVO Statement for the Use of Animals in Ophthalmic and Visual Research.

For all conditions, cross-linking included de-epithelialization and riboflavin (Vitamin B<sub>2</sub>, Streuli Pharma AG, Uznach, Switzerland) instillation for 20 minutes prior to UV irradiation by either a commercial device (CCL Vario, Peschke Meditrade GmbH, Huenenberg, Switzerland) or by a 365-nm UV LED emitter (LZC-00U600, LED Engin, San Jose, CA). The beam profile along a murine cornea of 3 mm diameter can be considered flat in both UV irradiation units. Riboflavin solutions were dissolved in PBS (Dulbecco's Phosphate Buffered Saline, Sigma-Aldrich Chemie GmbH Steinheim, Germany) to obtain concentrations of 0.1% and 0.27%.

### Anesthesia

Mice were anaesthetized with an intraperitoneal injection of ketamine (100 mg/kg, Ketalar Pfizer AG, Zurich, Switzerland) and xylazine (10 mg/kg, Bayer, Provet AG, Lyssach, Switzerland).

### De-epithelialization

The murine epithelium is more rigid than the human epithelium and therefore required a more aggressive procedure for removal. One drop of Tetracaine 1% (10 mg/mL, Novartis Pharma Schweiz AG, Bern, Switzerland) was placed on the cornea for 60 seconds and then removed with a surgical sponge (Sugi-Saugkeil, 17 × 8 mm, Dosch, Medizintechnik, Heidelberg, Germany). Then, one drop of 33% ethanol (in PBS) was administered for 180 seconds. The ethanol was removed with a surgical sponge and rinsed with PBS before the epithelium was gently scrapped off with the help of a surgical sponge.

### Riboflavin Application

One drop of the corresponding riboflavin solution was placed onto the cornea, stayed there for 20

minutes, and was then removed with a surgical sponge.

### UV Irradiation

The mice were placed in lateral position below the UV source and the entire cornea, including the limbus, was irradiated.

### Postop Treatment

Antibiotic ointment (Ofloxacin, Floxal 0.3%, Bausch & Lomb, Zug, Switzerland) was administered prophylactically onto the cornea directly after treatment and repeated twice daily until re-epithelialization in order to avoid infections.

### Re-epithelialization

In a subset of mice, the cornea was stained by fluorescein once daily to determine the speed of re-epithelialization.

### Euthanasia

A dose of pentobarbital (0.5 g/100 mL, 100 µL/animal, Thiopental, Inresa, Arzneimittel GmbH, Freiburg, Germany) was administered intraperitoneally.

## Analysis

### Optical Imaging

Corneas were examined with optical coherence tomography (OCT; Spectralis OCT, Heidelberg Engineering, Heidelberg, Germany) and slit-lamp at the following times: before CXL, immediately after CXL, and at 1, 2, 3, 7, 11, and 30 days after CXL.

### Histological Analysis

Histologic analysis was performed at 24 hours after CXL to evaluate keratocyte apoptosis and at 30 days after CXL to evaluate long-term changes. Histologic sections were also used to determine corneal thickness. For the preparation of semithin sections, the entire eyes were first prefixed in 3% paraformaldehyde for 1 hour. Then, corneas were isolated and further fixed in 2.5% glutaraldehyde in cacodylate buffer at pH 7.2 for 24 hours. Samples were washed twice in cacodylate buffer and stored in osmium tetroxide (1% OsO<sub>4</sub> in 0.1 M cacodylate buffer) for 1 hour before they were gradually dehydrated in ethanol (30%–100%). Samples were immersed in propylene oxide, propylene oxide, and epoxy (1:1), epoxy pure and epoxy mixture with starter, each step for at least 3 hours and finally embedded and polymerized at 60°C. Methylene blue staining was performed in 1-µm epoxy sections for morphological analysis.

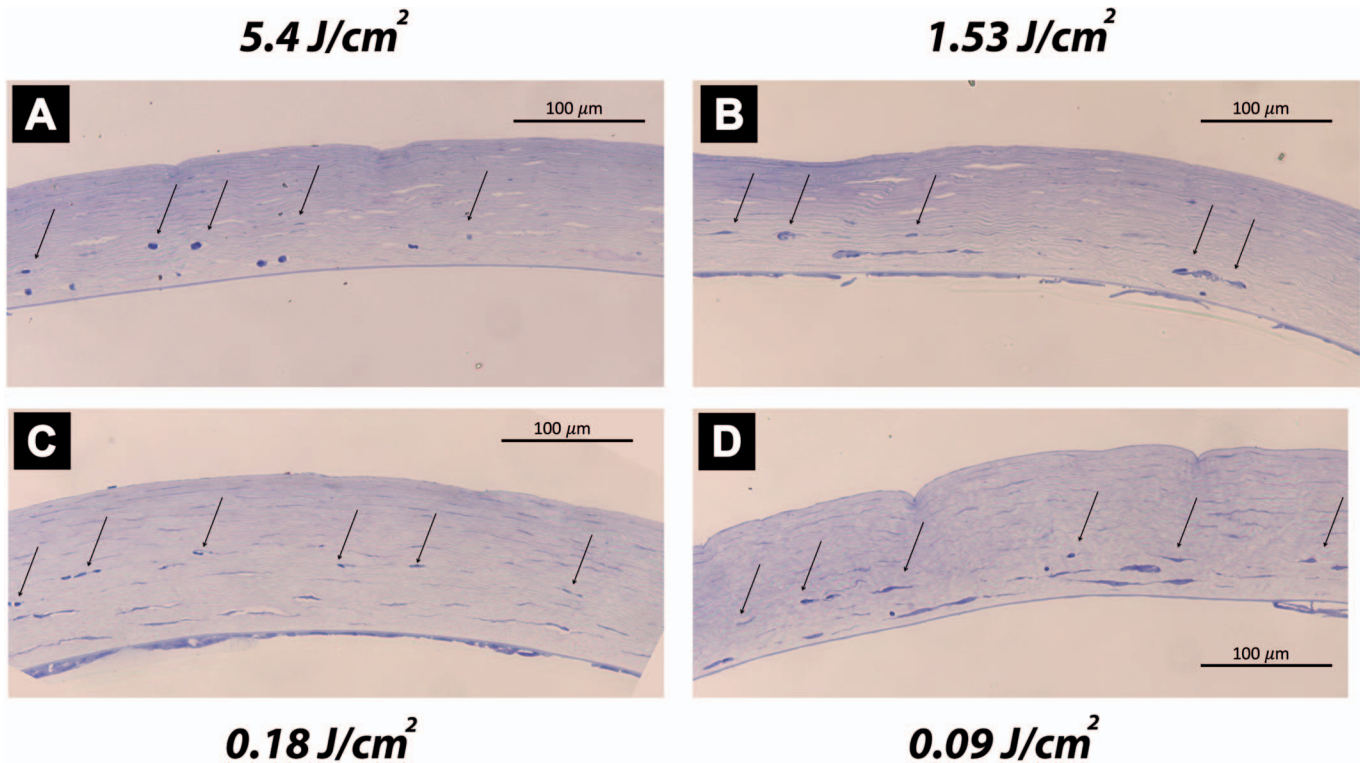


**Figure 1.** Histological analysis of the central cornea for different CXL protocols at 24 hours after treatment: 9 mW/cm<sup>2</sup>, 10 minutes, 0.5% riboflavin = 5.4 J/cm<sup>2</sup> (A), 9 mW/cm<sup>2</sup>, 2:50 minutes, 0.27% riboflavin = 1.53 J/cm<sup>2</sup> (B), 3 mW/cm<sup>2</sup>, 1 minute, 0.1% riboflavin = 0.18 J/cm<sup>2</sup> (C), 3 mW/cm<sup>2</sup>, 30 seconds, 0.1% riboflavin = 0.09 J/cm<sup>2</sup> (D). Keratocyte apoptosis in the central cornea reached a similar depth (*black arrows*) in all CXL protocols and was independent of irradiation time (30 seconds – 10 minutes) and UV fluence (0.09 – 5.4 J/cm<sup>2</sup>). However, keratocyte density was lower at higher UV fluences (A, B).

### Enzymatic Digestion

Enzymatic digestion was analyzed for comparison with our previous results on biomechanical 2-D stress-strain testing.<sup>29</sup> After complete re-epithelialization (3 days post-CXL), a subset of the mice ( $n = 18$ ) was sacrificed. The corneas from these mice were immediately extracted, and a corneal biopsy of 3 mm diameter taken. The samples were then subjected to enzymatic digestion by pepsin. Pepsin was used as it is a nonspecific endopeptidase that can break down both, collagens and proteoglycan core proteins. It is, therefore, more appropriate for assessing the effect of CXL than collagenase.<sup>34</sup> For the pepsin solution, 1 g pepsin (Roche Diagnostics AG, Rotkreuz, Switzerland) was dissolved in 100 mL 0.1 M HCL at pH 1.5. After immersion, the diameter of the corneal samples was measured every 3 hours during daytime.

### Statistical Analysis

The Student's *t*-test was used to determine statistical differences with enzymatic digestion. *P* values were corrected with the Bonferroni method in

order to correct for multiple testing. Confidence intervals of 95% were used.

## Results

### Histologic Analysis

Figure 1 shows corneal morphology at 24 hours after CXL with different treatment protocols. We observed a similar depth of central keratocyte apoptosis in nearly all corneas accounting for approximately 60% of the corneal thickness. Differences were observed in keratocyte density and peripheral repopulation, which both decreased with increasing fluence. Compared to riboflavin controls, the number of repopulating keratocytes decreased by  $-24 * \text{fluence} - 180 \text{ cells/mm}^2$  ( $R^2 = 0.718$ ) at 24 hours after treatment. Also, corneal swelling at 24 hours posttreatment correlated inversely with the fluence (see [Supplementary Fig. S1](#)). The swelling in less-irradiated corneas arises from de-epithelialization and wound healing. Strong-irradiated corneas have formed excessive cross-links that prevent swelling.

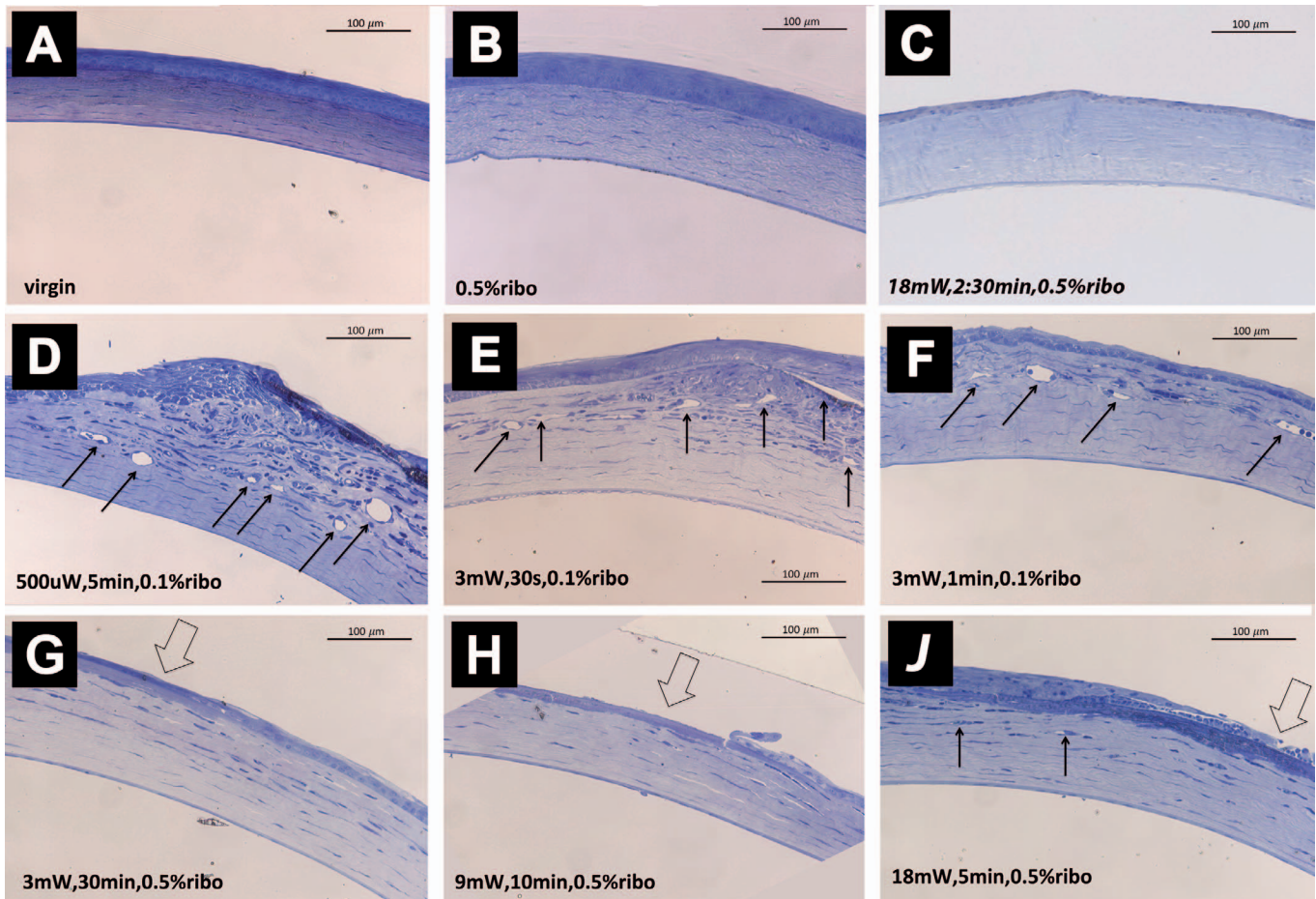


**Figure 2.** Histological analysis of the central cornea at 30 days after CXL. Control conditions virgin (A) and riboflavin-only (B) had no significant morphological alterations. Medium-fluence CXL ( $2.7 \text{ J/cm}^2$ ) reduced epithelial thickness, but maintained corneal transparency (C). Low-fluence CXL ( $\leq 0.18 \text{ J/cm}^2$ ) showed corneal haze and neovascularization (*small arrows*) due to strong immunological reactions (D–F). Standard-fluence CXL ( $5.4 \text{ J/cm}^2$ ) showed severe corneal scarring (*big arrows*) and no or only very minor neovascularization (*small arrows*; G–J).

Re-epithelialization in mice did not take significantly longer after CXL; however, epithelial morphology showed persistent abnormalities at 7 days after treatment in all eyes tested: we observed irregularities in corneal thickness and an absence of stratified squamous epithelial cell organization, indicating that the process of re-epithelialization was incomplete. However, while de-epithelialized only and riboflavin only corneas showed predominantly enlarged, hypertrophic basal epithelial cells and few wing and superficial epithelial cells, cross-linked corneas presented exclusively flat epithelial cells, resembling superficial cells (see [Supplementary Fig. S2](#)).

**Figure 2** presents corneal morphology at 30 days after CXL treatment. Different reaction mechanisms were observed: For fluences of  $5.4 \text{ J/cm}^2$  (panels G,

H, J), all corneas developed a central scar post CXL with abnormal epithelial cells. In the range from  $1.62$  to  $2.7 \text{ J/cm}^2$  (panel C), inconsistent effects were observed: either the corneas appeared transparent, but had a reduced epithelial thickness, or scar formation was observed (see also [Table 1](#)). For fluences lower or equal to  $0.18 \text{ J/cm}^2$  (panels D, E, F), corneas suffered from distinct immunological reactions: Increased numbers of activated keratocytes, polymorphonuclear cell infiltrates, extravasated erythrocytes, and neovascularization were observed. Riboflavin control corneas did not show significant cellular changes when compared to virgin controls, but showed increased corneal thickness.

At 30 days post CXL, controls and high-fluence CXL showed the thinnest corneas, while low-fluence



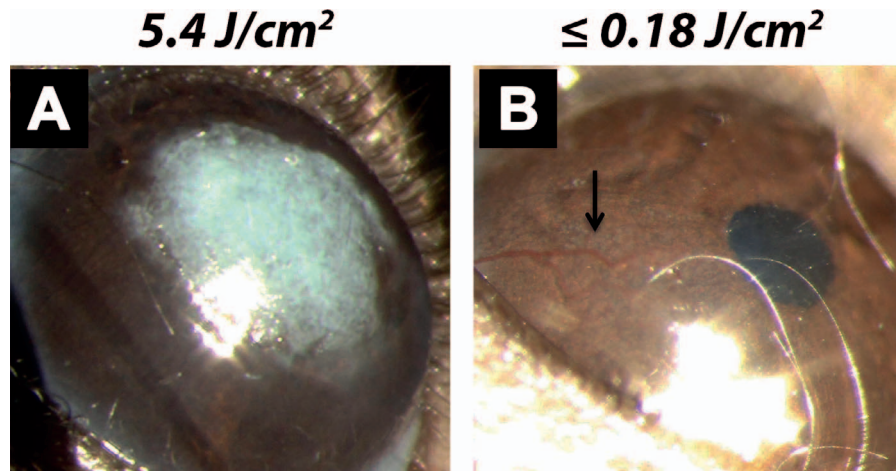


**Figure 3.** Stromal reactions 30 days posttreatment dependent on the CXL protocol used. With high-fluence CXL ( $5.4 \text{ J/cm}^2$ ) or increased oxygen availability (pCXL) a central stromal scar was observed (A); with low-fluence CXL ( $\leq 0.18 \text{ J/cm}^2$ ) or under hypoxia (caCXL) neovascularization (*arrow*) was observed (B).

CXL increased corneal thickness due to strong inflammatory reactions (see [Supplementary Fig. S1](#)).

#### Optical Imaging

In [Figure 3](#), two different manifestations at 30 days after CXL are shown: corneal scarring and neovascularization, depending on the fluence applied, but not on irradiance or the duration of UV irradiation.

[Figure 4](#) presents the follow-up with OCT and slit-lamp photographs at different times during the first 30 days after CXL in a cornea that developed a central scar. Unfortunately, the resolution of the OCT images was not sufficient to identify the demarcation line in murine corneas.

Immediately after the exposure, we noted increased stromal reflectivity due to riboflavin instillation. After an initial period (48–72 hours) of distinct stromal edema and partial re-epithelialization, the cornea was fully but irregularly re-epithelialized at 7 days post CXL. At 11 days post CXL, the stroma started to dehydrate irregularly locally in the zone with epithelial alteration. At 30 days post CXL, a stromal scar had formed at the region with epithelial irregularity that dehydrates at 11 days. After pCXL and caCXL, the cornea healed without complications and was transparent up to 3 weeks post CXL, before scar formation and neovascularization, respectively, occurred.

#### Enzymatic Digestion

The speed of enzymatic digestion correlated inversely with the biomechanical stiffness increase measured previously.<sup>29</sup> However, enzymatic digestion was less sensitive: At  $3 \text{ mW/cm}^2$ , an UV irradiation of

3 minutes or longer significantly ( $P < 0.001$ ) decreased the speed of pepsin digestion—on average by  $-6.3 \text{ }\mu\text{m/hour}$  or slower. An irradiation of 1 minute ( $-6.9 \text{ }\mu\text{m/hour}$ ) and caCXL ( $-10.3 \text{ }\mu\text{m/hour}$ ) reached the limit of detectability: significant differences were only found compared to virgin, but not to the riboflavin control. Thirty-second irradiation ( $-10.1 \text{ }\mu\text{m/hour}$ ) did not significantly slow down enzymatic digestion ( $P > 0.34$ ). Virgin controls had the fastest degradation rate ( $-11.4 \text{ }\mu\text{m/hour}$ ). Riboflavin controls were degraded at  $-7.5 \text{ }\mu\text{m/hour}$ . See [Table 2](#) for individual  $P$  values. Degradation speeds were calculated from 0 to 69 hours after immersion of the corneal biopsy into pepsin solution.

## Discussion

We tested several approaches to transfer the in vivo CXL treatment from the human to the mouse cornea and analyzed relevant tissue responses.

In a recently published study,<sup>29</sup> we showed that the increase in corneal biomechanical stiffness observed after CXL is more effective in mice than in humans. We were able to confirm this observation with our results obtained from enzymatic digestion.

There are major structural differences between human and murine corneas including collagen fibril orientation (orthogonal versus circumferential)<sup>35</sup> and the potential absence<sup>36</sup> or the minor development of Bowman's membrane in the murine cornea. Also, corneal collagen fibrils are slightly thicker with a higher packing density in mice (fibril diameter:  $35.5 \text{ nm}$ , interfibrillar spacing:  $49.7 \text{ nm}$ )<sup>37</sup> than in humans

## After CXL

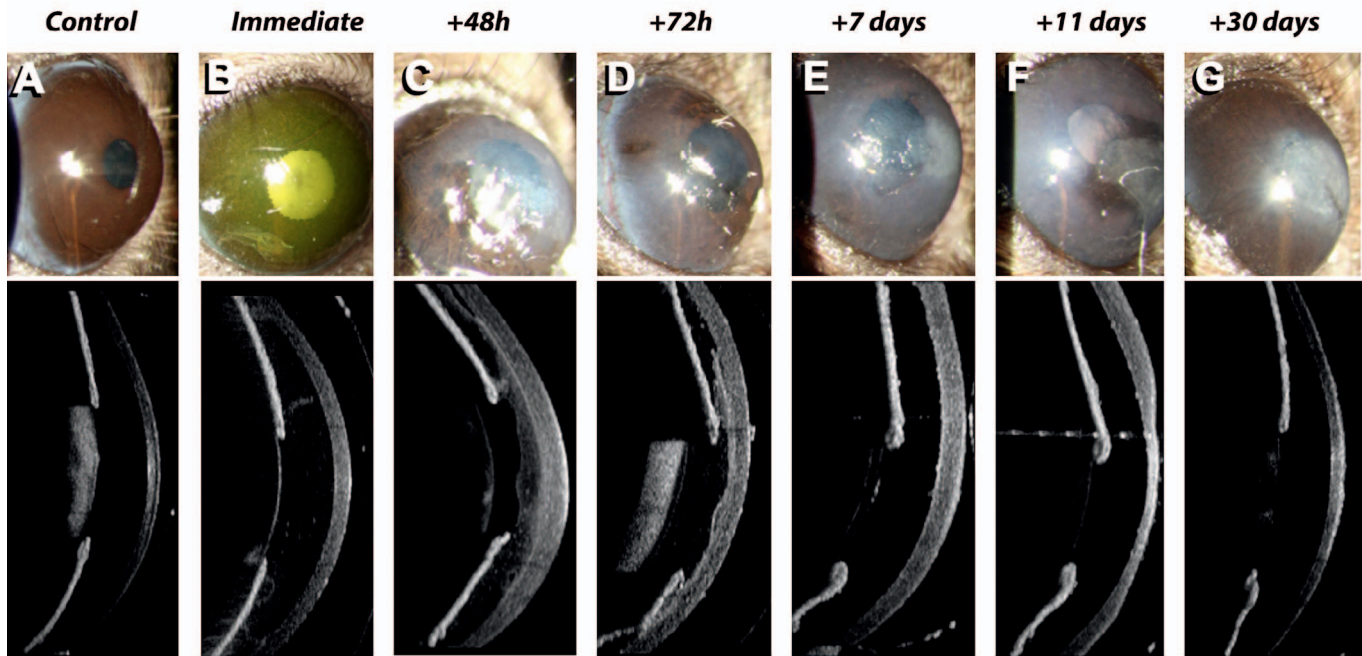


**Figure 4.** Slit lamp (*top row*) and AS-OCT (*bottom row*) images of a time course after CXL using UV fluences of  $5.4 \text{ J/cm}^2$ . Immediately after the exposure (B), we noted increased stromal reflectivity suggesting minor edema due to photosensitizer instillation. From 48 hours (C) to 72 hours (D) post CXL severe corneal edema and partial re-epithelialization was observed. At 7 days post CXL (E), the cornea was fully, but irregularly re-epithelialized. At 11 days post CXL (F), stromal edema decreased locally in the zone with irregular epithelium. At 30 days post CXL (G), a stromal scar had formed at the region with epithelial irregularity.

(fibril diameter: 30.8 nm, interfibrillar spacing: 55.3 nm).<sup>38</sup> Although the collagen packing is largely determined by the ratio of different collagen types, and the composition of the ECM proteins, differences in the collagen fibril packing cannot explain the

stronger CXL effect in mice: Crystallography experiments have shown that cross-links are not formed interfibrillarly.<sup>34</sup>

It is rather supposed that cross-links are formed within and between collagen molecules at the surface

**Table 2.** P Values Resulting from Statistical Analysis of Enzymatic Digestion in Murine Corneas after Riboflavin Instillation and UV Irradiation at  $3 \text{ mW/cm}^2$  and Different Durations

|              |              |             |              |              |               |
|--------------|--------------|-------------|--------------|--------------|---------------|
| 30 min–3 min | 30 min–1 min | 30 min–30 s | 30 min–caCXL | 30 min–ribo  | 30 min–virgin |
| 0.244        | 0.083        | 0.001       | 0.012        | 0.001        | 0.000         |
| 3 min–1 min  | 3 min–30 s   | 3 min–caCXL | 3 min–ribo   | 3 min–virgin | —             |
| 0.015        | 0.000        | 0.001       | 0.000        | 0.000        |               |
| 1 min–30 s   | 1 min–caCXL  | 1 min–ribo  | 1 min–virgin | —            | —             |
| 0.090        | 0.548        | 0.209       | 0.006        |              |               |
| 30 s–caCXL   | 30 s–ribo    | 30 s–virgin | —            | —            | —             |
| 0.225        | 0.516        | 0.343       |              |              |               |
| caCXL–ribo   | caCXL–virgin | —           | —            | —            | —             |
| 0.496        | 0.021        |             |              |              |               |
| ribo–virgin  | —            | —           | —            | —            | —             |
| 0.077        |              |             |              |              |               |

ribo, riboflavin control; virgin, virgin control.

of the fibrils, with and between proteoglycan core proteins and between the proteoglycan core proteins and the fibril surface.<sup>34</sup> The murine ECM differs from other mammals in terms that proteoglycans are undersulphated and that there is a higher proportion of dermatan sulfate to chondroitin sulfate and a lower content of keratan sulfate.<sup>39</sup> Some of these differences may be explained by the higher oxygen availability in the thin murine cornea, which favors the synthesis of chondroitin sulfate/dermatan sulfate rather than keratan sulfate. However, Western blot analysis demonstrated that keratan sulfate and chondroitin sulfate are not involved in the formation of cross-links during CXL<sup>40</sup> and hence these differences cannot explain the stronger effect of CXL in mice.

### The Role of Oxygen

In contrast, oxygen availability is an essential factor during CXL.<sup>33,41</sup> The thinner corneal thickness in murine corneas (137–191  $\mu\text{m}$ , center to periphery)<sup>30</sup> compared to human (552–604  $\mu\text{m}$ , center to periphery)<sup>31</sup> or porcine (666–714  $\mu\text{m}$ , center to periphery)<sup>42</sup> corneas allows—according to the Fick's law of diffusion—for an approximately 25 $\times$  faster oxygen diffusion, which potentially enhances the number of newly formed cross-links, as shown by our group recently.<sup>43</sup> Also, differences in the collagen orientation may affect the oxygen diffusion rate in the murine cornea. Oxygen is, therefore, considered to be responsible for the stronger stiffening effect after CXL in mice.

### Effect of UV Cross-linking

A number of post-CXL complications were observed in mice indicating the biological limits of the method in this particular animal model. Murine corneas treated with a fluence of 5.4 J/cm<sup>2</sup> developed a stromal scar, and if treated with a fluence of 0.18 J/cm<sup>2</sup> or lower, neovascularization and strong immunological reactions were observed. These reactions probably result from the higher oxygen availability and higher free radical density in the mouse cornea, but could potentially also arise from differences between the murine and human immune system.<sup>44</sup> Interestingly, corneal inflammation and haze only occurred in the anterior stroma where CXL initially caused keratocyte apoptosis, which indicates that unlike in clinical studies<sup>45</sup> these reactions probably do not arise from endothelial cell damage. A recent study applied CXL in a murine model of neovascularization and reported regression of the blood vessels 4 days

after treatment with 5.4 J/cm<sup>2</sup>.<sup>46</sup> These opposite biological responses at different UV fluences indicate a high sensitivity of CXL to treatment parameter modifications, which should be kept in mind also in the development of new CXL protocols for human patients. In this context, recent studies in rabbit corneas suggest that stromal cell death may be reduced by using a BKC-EDTA transepithelial CXL protocol.<sup>47,48</sup>

Corneal haze and scarring might indicate a too high degree of cross-linking: As soon as the collagen organization (fibril diameter, fibril spacing, degree of interconnection) changes distinctly, the cornea loses its transparency and its original mechanical properties. Permanent corneal haze and scarring after CXL has previously been observed in human corneas and occurred in patients with thin corneas<sup>49</sup> where a larger proportion of the cornea is cross-linked.<sup>49–51</sup> In our previous study, we showed that scar formation after CXL in mice did not change the biomechanical stiffness,<sup>29</sup> while in contrast neovascularization led to a complete loss of the previously increased corneal stiffness (unpublished data).

Corneal neovascularization typically results from inflammation (stromal keratitis) or persistent epithelial damage,<sup>52</sup> but has not been observed after CXL treatment in humans. Angiogenesis is rare as the cornea is an immunologically privileged site. On the molecular level, corneal vascularization requires both, upregulation of angiogenic factors—such as vascular endothelial growth factor (VEGF) and basic fibroblast growth factor (bFGF)—and downregulation of antiangiogenic factors—such as angiostatin and endostatin.<sup>52,53</sup> Matrix metalloproteinases (MMPs) may be involved in this process, as they can produce antiangiogenic factors, but also degrade the ECM and facilitate tissue proliferation.<sup>52</sup> Overexpression of MMPs has been observed in keratoconus disease<sup>54</sup> and therefore could indicate a pathway where CXL interferes with corneal gene expression.

Interestingly an increase of VEGF has been associated to hypoxia due to excessive contact lens wear.<sup>55</sup> Hypoxia also occurs during UV irradiation in CXL<sup>33</sup> and therefore may have triggered the upregulation of VEGF. Our experiments on caCXL and pCXL support this hypothesis, as only caCXL corneas (hypoxia) developed neovascularization, while pCXL corneas (increased oxygenation) did not, although in both conditions the same amount of UV fluence was applied. Adverse interactions between the contact lens and UV light can be ruled out as caCXL has already been performed in human

patients without any complications.<sup>13</sup> Reduced oxygen availability has also been reported in context with a reduced biomechanical stiffening effect.<sup>56,57</sup> While effective CXL may counteract neovascularization<sup>46</sup> due to the strong stiffening effect impeding the invasion of blood vessels, less-effective CXL protocols cannot prevent blood vessel invasion and face an excessive immune and wound healing reaction.

Although the speed of corneal re-epithelialization was not affected by CXL, the newly formed epithelium was different to that of the noncross-linked control corneas. While enlarged (hypertrophic) basal epithelial cells in virgin and riboflavin controls represent the normal response to wound healing (i.e., epithelium abrasion), the absence of those in cross-linked corneas indicates either an abnormal cell differentiation process, or that the low number of basal cells flattens to better cover the stroma. These abnormalities may come from a disturbed biochemical signaling of the corneal stroma due to the initially CXL-induced keratocyte apoptosis, or from potential damage to limbal stem cells by the UV irradiation. Nevertheless, earlier studies in rabbits have ruled out limbal damage after CXL, even when using the double UV fluence.<sup>58,59</sup> It is interesting to note that the keratocyte repopulation is much faster in mice than in humans (1 week versus 3 months).

Previously, we have shown that the biomechanical stiffness after CXL in mice could only increase up to a certain limit and that it starts to decrease with a fluence of 0.18 J/cm<sup>2</sup> or lower.<sup>16</sup> In the current study, we found that the fluence of 0.18 J/cm<sup>2</sup> corresponded to the fluence at which neovascularization was induced. We did not observe the depth of keratocyte apoptosis to correspond with the biomechanical stiffening effect, but rather with the density of surviving keratocytes in the stroma. This observation may be of importance for clinical studies that usually assume that the depth of the demarcation line is a measure of CXL efficacy.<sup>60</sup> It is, however, not well understood, if keratocyte apoptosis causes the demarcation line, or the actual formation of cross-links, and if the two regions are congruent.

Studying different CXL protocols in mice allowed us to analyze the physiological response of very strong and very weak CXL, as well as to identify the adequate range of UV fluence for CXL in mice. While our previous study<sup>29</sup> still showed a significant corneal stiffening effect, when the UV fluence was reduced to 0.09 J/cm<sup>2</sup>, the current study demonstrates that a fluence between 1.62 and 2.7 J/cm<sup>2</sup> causes least secondary effects, such as scar formation and

neovascularization. The stromal reaction following 0.54 J/cm<sup>2</sup> irradiation was strongly dependent on the treatment protocol and therefore was excluded from this range. Our study emphasizes the importance of identifying the correct therapeutic window of CXL, with respect to different corneal thicknesses and species. It also suggests that reducing the UV irradiance in thin corneas could potentially decrease the currently required minimal thickness of 400  $\mu$ m in human CXL.

The mouse may not be a good model to directly draw conclusions for human CXL treatment, particularly as no treatment protocol could be identified that was absent of any adverse corneal reaction. However, the application of the presented protocols for CXL in mice can be helpful in future basic research addressing cellular and molecular pathways associated to CXL treatment. Such studies potentially allow one to find a connection between the macroscopic physical behavior of the corneal tissue and its gene expression, and could also lead to the development of a genetic or pharmaceutical disease model for keratoconus.

## Acknowledgments

Supported by the Swiss National Science Foundation (A.H.), and the Gelbert Foundation (S.K., F.H.).

Disclosure: **S. Kling**, None; **A. Hammer**, None; **A. Conti**, None; **F. Hafezi**, None

\* Both authors contributed equally to the work presented here and should therefore be regarded as equivalent authors.

## References

1. Caporossi A, Mazzotta C, Baiocchi S, Caporossi T. Long-term results of riboflavin ultraviolet A corneal collagen cross-linking for keratoconus in Italy: the Siena eye cross study. *Am J Ophthalmol*. 2010;149:585–593.
2. Raiskup F, Spoerl E. Corneal crosslinking with riboflavin and ultraviolet A. Part II. Clinical indications and results. *Ocular Surface*. 2013;11:93–108.
3. Raiskup F, Spoerl E. Corneal crosslinking with riboflavin and ultraviolet A. I. Principles. *Ocular Surface*. 2013;11:65–74.

4. Wollensak G, Sporl E, Seiler T. [Treatment of keratoconus by collagen cross linking]. *Ophthalmologie*. 2003;100:44–49.
5. Hafezi F, Kanellopoulos, J, Wiltfang, R, Seiler, T. Corneal collagen crosslinking with riboflavin and ultraviolet A to treat induced keratectasia after laser in situ keratomileusis. *J Cataract Refract Surg*. 2007;33:2035–2040.
6. Kymionis GD, Kontadakis GA, Kounis GA, et al. Simultaneous topography-guided PRK followed by corneal collagen cross-linking for keratoconus. *J Refract Surg*. 2009;25:S807.
7. Richo O, Mavranakas N, Pajic B, Hafezi F. Corneal collagen cross-linking for ectasia after LASIK and photorefractive keratectomy: long-term results. *Ophthalmology*. 2013;120:1354–1359.
8. Hashemi H, Miraftab M, Seyedian MA, et al. Long-term results of an accelerated corneal cross-linking protocol 18mW/cm for the treatment of progressive keratoconus. *Am J Ophthalmol*. 2015;160:1164–1170.
9. Vinciguerra P, Rechichi M, Rosetta P, et al. High fluence iontophoretic corneal collagen cross-linking: in vivo OCT imaging of riboflavin penetration. *J Refract Surg*. 2013;29:376–377.
10. Raiskup F, Pinelli R, Spoerl E. Riboflavin osmolar modification for transepithelial corneal cross-linking. *Curr Eye Res*. 2012;37:234–238.
11. Hafezi F, Mrochen M, Iseli HP, Seiler T. Collagen crosslinking with ultraviolet-A and hypoosmolar riboflavin solution in thin corneas. *J Cataract Refract Surg*. 2009;35:621–624.
12. Mazzotta C, Traversi C, Caragiuli S, Rechichi M. Pulsed vs continuous light accelerated corneal collagen crosslinking: in vivo qualitative investigation by confocal microscopy and corneal OCT. *Eye*. 2014;28:1179–1183.
13. Jacob S, Kumar DA, Agarwal A, Basu S, Sinha P, Agarwal A. Contact lens-assisted collagen cross-linking (CACXL): a new technique for cross-linking thin corneas. *J Refract Surg*. 2014;30:366–372.
14. Wernli JSS, Spoerl E, Mrochen M. The efficacy of corneal cross-linking shows a sudden decrease with very high intensity UV light and short treatment time. *Invest Ophthalmol Vis Sci*. 2013;54.
15. Hafezi F. Limitation of collagen cross-linking with hypoosmolar riboflavin solution: failure in an extremely thin cornea. *Cornea*. 2011;30:917–919.
16. Hammer A, Richo O, Mosquera SA, Tabibian D, Hoogewoud F, Hafezi F. Corneal biomechanical properties at different corneal cross-linking (CXL) irradiances. *Invest Ophthalmol Vis Sci*. 2014;55:2881–2884.
17. Kling S, Richo O, Hammer A, et al. Increased biomechanical efficacy of corneal cross-linking in thin corneas due to higher oxygen availability. *J Refract Surg*. 2015;31:840–846.
18. Spoerl E, Wollensak G, Seiler T. Increased resistance of crosslinked cornea against enzymatic digestion. *Curr Eye Res*. 2004;29:35–40.
19. Wollensak G, Iomdina E. Biomechanical and histological changes after corneal crosslinking with and without epithelial debridement. *J Cataract Refract Surg*. 2009;35:540–546.
20. Wollensak G, Spoerl E, Seiler T. Riboflavin/ultraviolet-A-induced collagen crosslinking for the treatment of keratoconus. *Am J Ophthalmol*. 2003;135:620–627.
21. Kling S, Ginis H, Marcos S. Corneal biomechanical properties from two-dimensional corneal flap extensometry: application to UV-riboflavin cross-linking. *Invest Ophthalmol Vis Sci*. 2012;53:5010–5015.
22. Kling S, Remon L, Pérez-Escudero A, Merayo-Llves J, Marcos S. Corneal biomechanical changes after collagen cross-linking from porcine eye inflation experiments. 2010;51:3961–3968.
23. Kling S, Marcos S. Contributing factors to corneal deformation in air puff measurements. *Invest Ophthalmol Vis Sci*. 2013;54:5078–5085.
24. Ambrósio Jr R, Ramos I, Luz A, et al. Dynamic ultra high speed Scheimpflug imaging for assessing corneal biomechanical properties. *Revista Brasileira de Oftalmologia*. 2013;72:99–102.
25. Raiskup F, Theuring, A, Pillunat LE, Spoerl E. Corneal collagen crosslinking with riboflavin and ultraviolet-A light in progressive keratoconus: ten-year results. *J Cataract Refract Surg*. 2015;41:41–46.
26. Wang N, Butler JP, Ingber DE. Mechanotransduction across the cell surface and through the cytoskeleton. *Science*. 1993;260:1124–1127.
27. Vogel V. Mechanotransduction involving multimodular proteins: converting force into biochemical signals. *Annu Rev Biophys Biomol Struct*. 2006;35:459–488.
28. Humphrey JD, Dufresne ER, Schwartz MA. Mechanotransduction and extracellular matrix homeostasis. *Nat Rev Mol Cell Biol*. 2014;15:802–812.
29. Hammer A, Kling S, Boldi MO, et al. Establishing corneal cross-linking with riboflavin and UV-A in the mouse cornea in vivo: biomechanical

- analysis. *Invest Ophthalmol Vis Sci.* 2015;56: 6581–6590.
30. Henriksson JT, McDermott AM, Bergmanson JP. Dimensions and morphology of the cornea in three strains of mice. *Invest Ophthalmol Vis Sci.* 2009;50:3648–3654.
  31. Tomlinson A. A clinical study of the central and peripheral thickness and curvature of the human cornea. *Acta Ophthalmologica.* 1972;50:73–82.
  32. Spoerl E, Mrochen M, Sliney D, Trokel S, Seiler T. Safety of UVA-riboflavin cross-linking of the cornea. *Cornea.* 2007;26:385–389.
  33. Kamaev P, Friedman MD, Sherr E, Muller D. Photochemical kinetics of corneal cross-linking with riboflavin. *Invest Ophthalmol Vis Sci.* 2012; 53:2360–2367.
  34. Hayes SK-LC, Boote C, Young RD, et al. The effect of riboflavin/UVA collagen cross-linking therapy on the structure and hydrodynamic behaviour of the ungulate and rabbit corneal stroma. *Plos One.* 2013;8:e52860.
  35. Keith M, Meek CB. The use of X-ray scattering techniques to quantify the orientation and distribution of collagen in the corneal stroma. *Prog Retinal Eye Res.* 2009;28:369–392.
  36. Hazlett LD. Corneal and ocular surface histochemistry. *Prog Histochem Cytochem.* 1993;25: III–60.
  37. Quantock AJ, Dennis S, Adachi W, et al. Annulus of collagen fibrils in mouse cornea and structural matrix alterations in a murine-specific keratopathy. *Invest Ophthalmol Vis Sci.* 2003;44: 1906–1911.
  38. Leonard DW, Meek, KM. Refractive indices of the collagen fibrils and extrafibrillar material of the corneal stroma. *Biophys J.* 1997;72:1382.
  39. Parfitt GJ, Pinali C, Young RD, Quantock AJ, Knupp C. Three-dimensional reconstruction of collagen–proteoglycan interactions in the mouse corneal stroma by electron tomography. *J Struct Biol.* 2010;170:392–397.
  40. Zhang Y, Conrad AH, Conrad GW. Effects of ultraviolet-A and riboflavin on the interaction of collagen and proteoglycans during corneal cross-linking. *J Biol Chem.* 2011;286:13011–13022.
  41. Richoz O, Hammer A, Tabibian D, Gatzoufas Z, Hafezi F. The biomechanical effect of corneal collagen cross-linking (CXL) with riboflavin and UV-A is oxygen dependent. *Trans Vis Sci Tech.* 2013;2.
  42. Faber C, Scherfig E, Prause JU, Srensen KE. Corneal thickness in pigs measured by ultrasound pachymetry in vivo. *Scand J Lab Animal Sci.* 2008;35:39–43.
  43. Kling S, Richoz O, Hammer A, et al. Increased biomechanical efficacy of corneal cross-linking in thin corneas due to higher oxygen availability. *J Refract Surg.* 2015;31:840–846.
  44. Mestas J, Hughes CC. Of mice and not men: differences between mouse and human immunology. *J Immunol.* 2004;172:2731–2738.
  45. Gokhale NS. Corneal endothelial damage after collagen cross-linking treatment. *Cornea.* 2011;30: 1495–1498.
  46. Bock F, Tóth G, Szentmary N, Bucher F, Cursiefen C. Corneal crosslinking with ultraviolet-A and riboflavin in a murine model of corneal neovascularization. *Invest Ophthalmol Vis Sci.* 2015;56:4517.
  47. Armstrong BK, Lin MP, Ford MR, et al. Biological and biomechanical responses to traditional epithelium-off and transepithelial riboflavin-UVA CXL techniques in rabbits. *J Refract Surg.* 2013;29:332–341.
  48. Torricelli AA, Ford MR, Singh V, Santhiago MR, Dupps WJ, Wilson SE. BAC-EDTA trans-epithelial riboflavin-UVA crosslinking has greater biomechanical stiffening effect than standard epithelium-off in rabbit corneas. *Exp Eye Res.* 2014;125:114–117.
  49. Raiskup FHA, Spoerl E. Permanent corneal haze after riboflavin-UVA-induced cross-linking in keratoconus. *J Refract Surg.* 2009;25:S824–S828.
  50. Kato N, Konomi K, Saiki M, et al. Deep stromal opacity after corneal cross-linking. *Cornea* 2013; 32:895–898.
  51. Koppen C, Vryghem JC, Gobin L, Tassignon MJ. Keratitis and corneal scarring after UVA/riboflavin cross-linking for keratoconus. *J Refract Surg.* 2009;25:S819–S823.
  52. Chang JH, Gabison EE, Kato T, Azar DT. Corneal neovascularization. *Curr Opin Ophthalmol.* 2001;12:242–249.
  53. Folkman JSY. Angiogenesis. *J Biol Chem.* 1992; 167:10931–10934.
  54. Balasubramanian SA, Mohan S, Pye DC, Willcox MDP. Proteases, proteolysis and inflammatory molecules in the tears of people with keratoconus. *Acta Ophthalmologica.* 2012;90:e303–e309.
  55. Mastuyugin V, Mosaed S, Bonazzi A, Dunn MW, Schwartzman ML. Corneal epithelial VEGF and cytochrome P450 4B1 expression in a rabbit model of closed eye contact lens wear. *Curr Eye Res.* 2001;23:1–10.
  56. Richoz O, Hammer A, Tabibian D, Gatzoufas Z, Hafezi F. The biomechanical effect of corneal collagen cross-linking (CXL) with riboflavin and

- UV-A is oxygen dependent. *Trans Vis Sci Tech.* 2013;2:6.
57. Kling S, Richoz O, Hammer A, et al. Increased biomechanical efficacy of corneal cross-linking in thin corneas due to higher oxygen availability. *J Refract Surg.* 2015;31:840–846.
58. Wollensak G, Mazzotta C, Kalinski T, Sel S. Limbal and conjunctival epithelium after corneal cross-linking using riboflavin and UVA. *Cornea.* 2011;30:1448–1454.
59. Richoz O, Tabibian D, Hammer A, Majo F, Nicolas M, Hafezi F. The effect of standard and high-fluence corneal cross-linking (CXL) on cornea and limbus. *Invest Ophthalmol Vis Sci.* 2014;55:5783–5787.
60. Kymionis GD, Tsoulnaras KI, Grentzelos MA, et al. Evaluation of corneal stromal demarcation line depth following standard and a modified-accelerated collagen cross-linking protocol. *Am J Ophthalmol.* 2014;158:671–675.